Sensors & Transducers, Vol. 237, Issue 9-10, September-October 2019, pp. 80-87

www.sensorsportal.com

Sensors & Transducers

Published by IFSA Publishing, S. L., 2019
http://www.sensorsportal.com

Novel and Cost-efficient Sensors for the Concentration Measurement of Ammonia and Ammonium Nitrate Particles

*** Mohamed Lamine BOUKHENANE, Nathalie REDON, Jean-Luc WOJKIEWICZ, Caroline DUC and Patrice CODDEVILLE**

IMT Lille Douai, Univ. Lille, Atmospheric Sciences and Environmental Engineering Laboratory, (SAGE), 59000 Lille, France
Tel.: +33327712296
E-mail: mohamed-lamine.boukhenane@imt-lille-douai.fr

Received: 30 August 2019 /Accepted: 27 September 2019 /Published: 30 November 2019

Abstract: In the presence of high concentrations of ammonia and nitric acid gas, the formation of ammonium nitrate particles (NH_4NO_3) is well established at low temperatures. As a result, high concentrations of ammonium nitrate particles are usually observed during the spring and winter period. Due to its semi-volatile nature, the measurement of ammonium nitrate with classical methods based on filter sampling (sampling time ≥ 24 h) introduce severe artifacts. Thus, the main objective of this study is to develop new low-cost sensors able to measure simultaneously and selectively the concentration of ammonium nitrate particles and its gaseous precursor ammonia. Sensors combine two surfaces which are sensitive to ammonia and based on polyaniline nano-composites materials. The mass concentration of ammonium nitrate is determined by measuring the concentration of the ammonia released by heating one of the sensitive surfaces. Sensors show a response to gaseous ammonia at concentrations less than 20 ppb with sensitivity around 0.3 %.ppb^{-1}, and the limit of detection of sensors to ammonium nitrate particles is around 270 µg.m^{-3} with a sensitivity of 0.0014 %.µg^{-1}.m^3.

Keywords: Air quality sensors, Ammonium nitrate particles, Gaseous ammonia, Conductive polymer, Polyaniline.

1. Introduction

Gaseous ammonia is one of the main nitrogen compounds found in the troposphere after N_2 and N_2O [1-2]. Over 80 % of ammonia emissions come from agricultural activities (livestock, fertilizers, soils…) [3]. Ammonia emissions are not considered as a regulated pollutant in the ambient air in Europe, although they are responsible of many adverse effects on the environment including soil acidification and aquatic eutrophication [4]. In addition, ammonia gas can contribute to particulate matter formation by reacting with acidic species (H_2SO_4, HNO_3, HCl) leading to the formation of secondary aerosols [5].

Atmospheric particulate matter, particularly PM_{10} and $PM_{2.5}$ have a significant impact on human health by causing many respiratory diseases (asthma, chronic obstructive pulmonary disease, and lung cancer) [6]. The spatial and temporal variability of $PM_{2.5}$ composition and mass concentration was studied by many authors [7–10]. Usually, the higher concentrations of particles are observed during the spring and winter period [11]. Indeed, according to a study conducted by Sharma, *et al.* [12] at Delhi, India,

during January 2013 to May 2014, the average mass concentration of $PM_{2.5}$ was estimated at 196 $\mu g.m^{-3}$ during winter months (January and December) and at 84 $\mu g.m^{-3}$ during the summer period. In another study carried out by Tao, *et al.* [13] in Chengdu, China, for a period of one month in every season during 2009–2010, the highest seasonal average of $PM_{2.5}$ concentrations was observed in the winter (225.5±73.2 $\mu g.m^{-3}$) and the lowest in the summer (113.5±39.3 $\mu g.m^{-3}$). In Europe, the mass concentrations of $PM_{2.5}$ are often lower than in India and East Asia. The concentration levels ranged between 8 $\mu g.m^{-3}$ and 53 $\mu g.m^{-3}$ in the winter and from 10 $\mu g.m^{-3}$ to 25 $\mu g.m^{-3}$ in the spring [14-15]. However, in some regions, it is possible to reach higher daily concentrations of $PM_{2.5}$, exceeding 80 $\mu g.m^{-3}$.

In addition, several species enter into the composition of $PM_{2.5}$. Among them, sulfate (SO_4^{2-}), nitrate (NO_3^-) and ammonium (NH_4^+) are the predominant water-soluble ionic species of $PM_{2.5}$. They represent approximately 20-40 % of $PM_{2.5}$ [14-15]. Wang, *et al.* [16] reported that the average mass concentrations of NO_3^-, SO_4^{2-} and NH_4^+ species measured from 8-28 November 2011 in Beijing, China, are respectively: 14.7±11.2 $\mu g.m^{-3}$, 12.2±9.63 $\mu g.m^{-3}$, and 9.13±7.26 $\mu g.m^{-3}$. Furthermore, Jiang, *et al.* [17] estimated respectively their annual mass concentrations from 2014 to 2015 in Zhengzhou, China, at: 20 $\mu g.m^{-3}$, 25 $\mu g.m^{-3}$ and 15 $\mu g.m^{-3}$.

The formation of ammonium nitrate particles NH_4NO_3 becomes possible in areas characterized by high ammonia and nitric acid concentrations at low temperatures following full neutralization of acidic sulfate. The process is described by the reversible reaction at temperatures below 170°C [18]:

$$NH_3\,(g) + HNO_3\,(g) \leftrightarrow NH_4NO_3\,(s, aq)$$

The reaction equilibrium and ammonium nitrate state depend on the temperature and relative humidity. Due to its semi-volatile nature, ammonium nitrate can evaporate at ambient temperatures ≥ 20°C [19]. Furthermore, nitric acid is mainly formed by oxidation of NO_2 by OH radicals (NO_2+OH) during the daytime or by hydrolysis of dinitrogen pentoxide (N_2O_5) during the nighttime [20].

According to Tao, *et al.* [21], the neutralization of nitrate by ammonia to obtain ammonium nitrate particles becomes evident at $[NH_4^+]/[SO_4^{2-}] > 2$. This molar ratio of ammonium to sulfate can be obtained during the spring and winter period.

Since a long time, the measurement of atmospheric particles is carried out with the classical method which is based on filter sampling by using denuders and filterpack, followed by laboratory analysis (Ionic Chromatography, gravimetric analysis…). However this technique can introduce severe artifacts and a loss of semi-volatile particles such as ammonium nitrate [22].

On the other hand, the continuous monitoring of aerosol composition and their mass concentration or size distribution can be done with many instruments such as ACSM (*Aerosol Chemical Speciation Monitor*), AMS (*Aerosol Mass Spectrometer*) and TEOM (*Tapered element oscillating microbalance*). However, these instruments are relatively expensive, bulky, and require highly qualified staff.

It is not easy to determine the mass concentration of the particulate form of ammonium nitrate with only the chemical speciation of particles. An alternative method to estimate its concentration is the revised IMPROVE method (*Interagency Monitoring of Protected Visual Environments*). This method is used for the reconstruction of $PM_{2.5}$ mass, by estimating the extinction coefficient (b_{ext}) of the particles. Assuming that SO_4^{2-} and NO_3^- ions are fully neutralized by NH_4^+ in the forms of $(NH_4)_2SO_4$ and NH_4NO_3 respectively, it is possible to estimate the concentration of NH_4NO_3 by multiplying the NO_3^- mass by a factor of 1.29 [16, 23].

Moreover, the most particle sensors rely on an optical sensing principle and don't give any information on the chemical nature of the particles. The mass concentration is estimated from count data, by using an ideal particle (size). Thus, the development of specific sensors for both particles and gas measurement could be complicated.

As known, conductive polymers are widely used to develop gas sensors among them, ammonia sensors based on polyaniline (PANI). Besides the versatility of their use because of their easy synthesis and their good environmental stability, polyaniline polymers are less expensive, they have tunable electrical properties and they are sensitive to many gaseous compounds at room temperature [24]. In the present work, we propose a new low-cost sensor based on polyaniline nanocomposites for simultaneous and selective measurement of the concentration of ammonium nitrate particles and its gaseous precursor ammonia in ambient air.

2. Materials & Methods

2.1. Operating Principle

Sensor consists of two ammonia sensitive surfaces based on polyaniline nanocomposites. One of the surfaces is heated by a thermoregulation system in a controlled volume at temperature close to 30 °C in order to initiate the evaporation of ammonium nitrate particles into ammonia and nitric acid. With the heated surface, the total concentration of ammonia including the released ammonia after the thermal decomposition will be determined. Sensing mechanism of ammonia gas with polyaniline is described in the literature and given in Fig. 1 [25]. While, the unheated surface measures only the concentration of ammonia already present in the air. The difference between both concentrations of ammonia determined with both sensitive surfaces will be correlated to ammonium nitrate concentration.

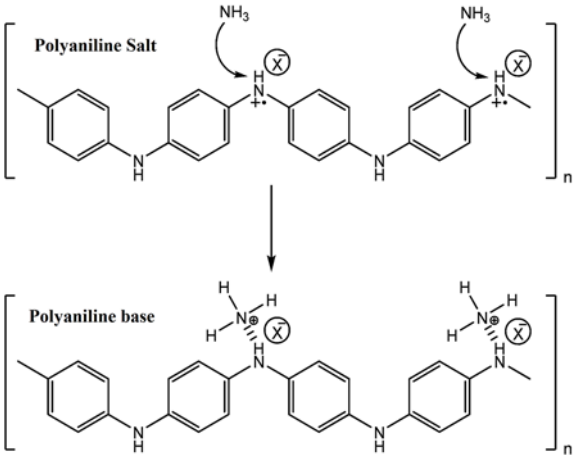

Fig. 1. Sensing mechanism of ammonia gas with polyaniline [25].

2.2. Preparation of the Sensor

In this work, polyaniline (PANI) based nanocomposite materials were prepared by mixing PANI with polyurethane matrix (PU) with two mass ratios of PANI: 50 % and 75 % for $PANI_{50wt\%}$/PU (PU1) and $PANI_{75wt\%}$/PU (PU2) materials respectively. The polymer matrix has been added in order to improve the mechanical properties of sensitive surfaces. Polyaniline emeraldine base (PANI-EB) was protonated by camphorsulfonic acid (CSA) with doping rate of 50 % leading to the formation of conductive polyaniline emeraldine salt (PANI-ES). PANI and CSA acid in powder form were first mixed and ground in a mortar and then dissolved in Dichloroacetic acid (DCAA) which can be considered as solvent and secondary dopant of polyaniline. In order to ensure a good doping of polyaniline, the solution was stirred for one week. At the same time, PU solution was prepared by dissolving a thermoplastic polyurethane (Covestro Desmopan® DP 6065A Polyurethane) in Dichloroacetic acid. The final solutions of PANI and PU were mixed and sonicated for 1h. The synthesis method of these materials is well described in previous works [26-27].

Solutions were drop-casted onto interdigitated gold electrodes patterned on ceramic substrate (Synkera) and then dried in a vacuum oven for 7 days at 100 °C. The film thickness was around 1 µm. Three sensors of each composite were tested under controlled conditions in order to study the reproducibility.

2.3. Particles Generation and Decomposition

An experimental bench of generation and decomposition of ammonium nitrate particles under controlled conditions has been especially developed for this project in order to determine the sensor response in presence of ammonium nitrate particles. Particles generation is ensured by nebulization of ammonium nitrate solution with AGK 2000 (PALAS). The particles are then dried with Nafion membrane "Perma Pure" (length: 60 cm). The relative humidity measured after particles drying is fixed at 45 %. The mass concentration of ammonium nitrate particles is determined before starting the thermal decomposition by using TEOM series 1400a operating at 30 °C in order to reduce the particle loss in the filter and the particles size distribution is done by FIDAS 200 particle counter. Particle diameter is comprised between 0.1 µm and 0.4 µm. The mass concentration of the generated particles depends on several parameters including the concentration of ammonium nitrate solution, the nebulization flow and the dilution rate. Fig. 2 gives an example of the average mass concentration of particles obtained during 15 minutes at different concentrations of ammonium nitrate solution without dilution and with the nebulization flow fixed at 3 L/min. The stability of the generation is comprised between ±7 % and ±15 %.

The thermal decomposition of particles is carried out using a climatic chamber heated at 30 °C to 50 °C when the sensitive surfaces are placed in the exposure chamber (0.5 L). Particles decomposition will be ensured with an autonomous thermoregulation system when the detection principle is validated.

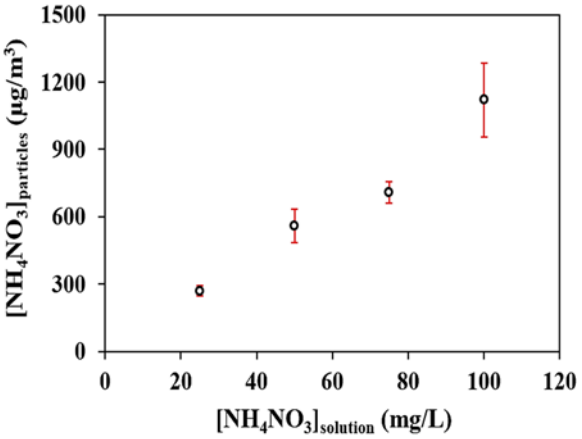

Fig. 2. Examples of the mass concentration of NH_4NO_3 particles obtained at different concentrations of ammonium nitrate solution.

2.4. Material Characterization

The morphology of PANI/PU materials was visualized by Scanning Electron Microscopy (SEM) (JEOL JCM-6000Plus). Thus, the solutions were deposited on polyamide and dried for 7 days at 100 °C in vacuum oven. The obtained films have undergone a gold sputtering before SEM analysis.

On the other hand, the electrical conductivity of materials was measured by four point probes technique by using Hall measurements in Van Der Pauw configuration (Ecopia HMS-5300). The films were prepared in the manner described above. The film thickness was estimated at 2 µm. All

measurements of film thickness were carried out using an optical profilometer (STIL). The electrical conductivity of the synthesized materials is given in Table 1 (average value of three samples).

Table 1. The electrical conductivity of PANI based nanocomposite films

Sample	wt % PANI	Dopant	Conductivity (S/cm)
PU1	50	CSA	0.17 ± 0.04
PU2	75	CSA	30 ± 3.60

3. Results and Discussion

3.1. Detection of Ammonia

Firstly, sensors were characterized in the presence of ammonia under controlled conditions in the ppb range in order to be able to detect lower concentrations of ammonia and ammonium nitrate in the ambient air. Sensors response to ammonia gas is determined as a relative variation of the resistance **(R)** of the sensor during exposure to ammonia compared to the initial value (R_0) under purified air: Response (%) = $[(R-R_0)/R_0]\times100$. Fig. 3 shows the relative response of $PANI_{75\ wt\%}$/PU sensors to ammonia gas at concentration range less than 60 ppb (RT/50 % RH) during 30 minutes of exposure to ammonia followed by purified air during 30 minutes. The red curve represents ammonia concentration measured in the exposure chamber with ammonia analyzer "PICARRO" model G2103.

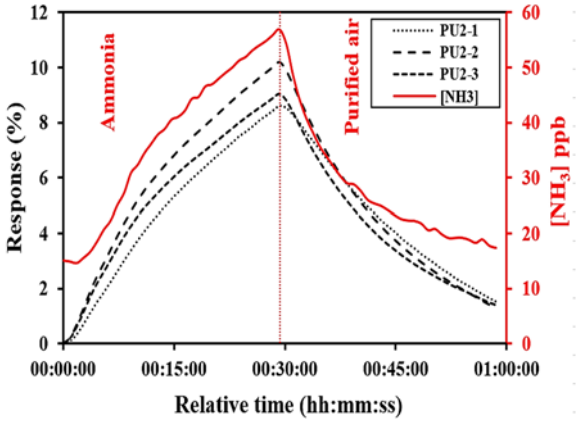

Fig. 3. Response of $PANI_{75\ wt\%}$/PU (PU2) sensors to ammonia at concentrations less than 60 ppb (RT/50 % RH).

As shown in Fig. 3, sensors presented a response to ammonia variations in agreement with the concentration measured with ammonia analyzer at concentrations below 60 ppb.

The calibration curve of $PANI_{50\ wt\%}$/PU and $PANI_{75\ wt\%}$/PU sensors obtained by plotting their relative response as a function of ammonia concentration measured by the analyzer is given in Fig. 4. Sensors showed a linear response to ammonia in the ppb range with very low limit of detection (<20 ppb). Moreover, the best sensitivity to ammonia (slope of the calibration curve) is obtained with $PANI_{50\ wt\%}$/PU sensors (0.33 %.ppb^{-1}) compared to 0.2 %.ppb^{-1} in the case of $PANI_{75\ wt\%}$/PU sensors. The good sensitivity of $PANI_{50\ wt\%}$/PU sensors could be explained by their structured topography as demonstrated with the SEM images given in Fig. 5A. This structure improves the adsorption capacity of the materials at low concentrations of gas. These sensitivities can be considered important in comparison with ammonia sensors performances presented in literature (Table 2).

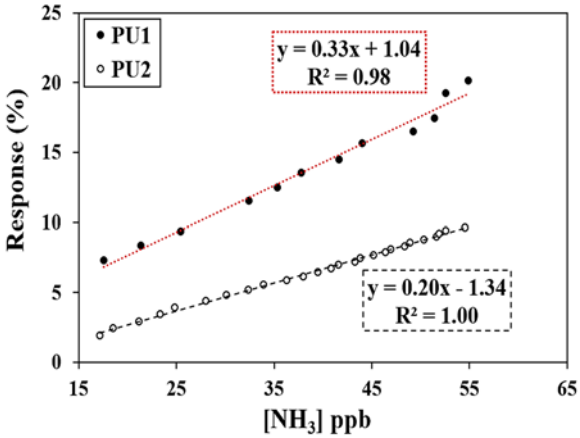

Fig. 4. Calibration curve of $PANI_{50\ wt\%}$/PU (PU1) and $PANI_{75\ wt\%}$/PU (PU2) sensors (RT/50 % RH).

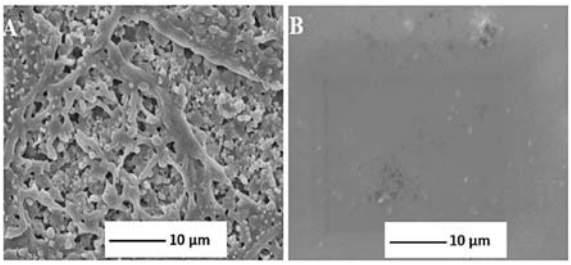

Fig. 5. SEM images of $PANI_{50\ wt\%}$/PU (A) and $PANI_{75\ wt\%}$/PU (B) materials.

Sensors repeatability and reproducibility were also studied. Fig. 6 gives the average sensitivity obtained during four exposures for 3 sensors of each material. Sensors sensitivity can be considered stable during four consecutive exposures to low ammonia concentrations. Similar sensitivities were also obtained by the three sensors of the same material. In order to evaluate sensors reproducibility, we calculated the variability of their average sensitivity given by the standard deviation multiplied by 100 and

divided by the average value of sensitivity. We determined a variability of 24 % and 8 % for $PANI_{50\ wt\%}/PU$ and $PANI_{75\ wt\%}/PU$ sensors respectively. A sensor with a variability lower than 25 %, can be considered as reproducible.

Table 2. Comparison of the sensing properties of the studied sensors with other PANI based sensors of ammonia.

Material	D_L	Sensitivity (%.ppb^{-1})	Ref
PANI (MW)	7 ppb	0.015	[30]
PANI/SnO_2	1.8 ppm	0.026	[31]
PANI/WO_3	5 ppm	1.25×10^{-3}	[32]
PANI/TiO_2	23 ppm	4.3×10^{-3}	[33]
PANI/TiO_2	45 ppb	0.065	[34]
$PANI_{0.01M}$/SBS	100 ppb	0.014	[35]
PANI/CNT	200 ppb	0.05	[36]
PANI/Graphene	1 ppm	0.011	[37]
PANI/PET	5 ppm	2.6×10^{-4}	[38]
PANI/TiO_2/Cellulose	10 ppm	2.4×10^{-3}	[39]
$PANI_{50\ wt\%}/PU$	<20 ppb	0.33	This
$PANI_{75\ wt\%}/PU$	<20 ppb	0.2	work

D_L: Detection limit; MW: Microwave synthesis.

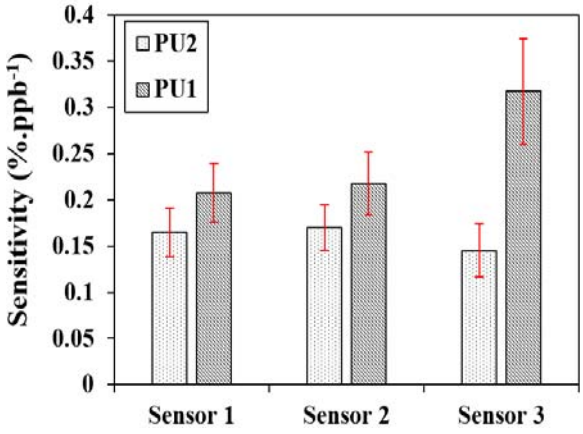

Fig. 6. Average sensitivity of $PANI_{50\ wt\%}/PU$ (PU1) and $PANI_{75\ wt\%}/PU$ (PU2) sensors during four exposures (RT/50 % RH).

The effect of temperature on sensors sensitivity was also studied in order to ensure that sensors can respond to the released ammonia at temperatures between 30 °C and 50 °C. Fig. 7 gives the average sensitivity obtained during four exposures for 3 sensors based on $PANI_{75\ wt\%}/PU$ as a function of three temperatures: 25 °C, 30 °C and 40 °C. Sensors sensitivity decreases with increase in temperature. A sensitivity of 0.03 %.ppb^{-1} was obtained at 40 °C compared to 0.2 %.ppb^{-1} at 25°C. Similar results was also obtained by Kukla, *et al.* [28]. This decrease of the sensitivity with the increase of temperature can be partially explained by the promotion of the desorption mechanism under the effect of the temperature.

The temperature dependence of the electrical conductivity of $PANI_{50\ wt\%}/PU$ and $PANI_{75\ wt\%}/PU$ materials between 25 °C and 68 °C is given in Fig. 8.

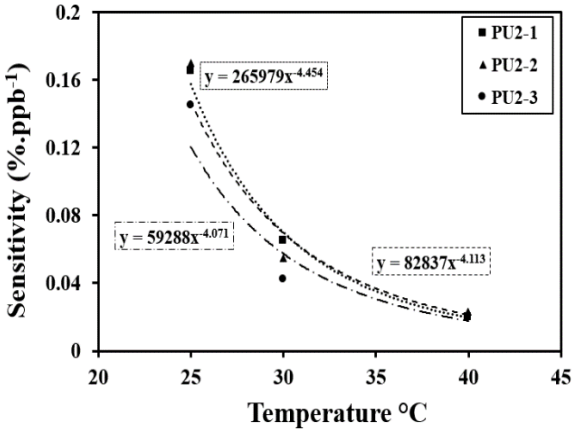

Fig. 7. The effect of temperature on the sensitivity to ammonia of sensors based on $PANI_{75\ wt\%}/PU$.

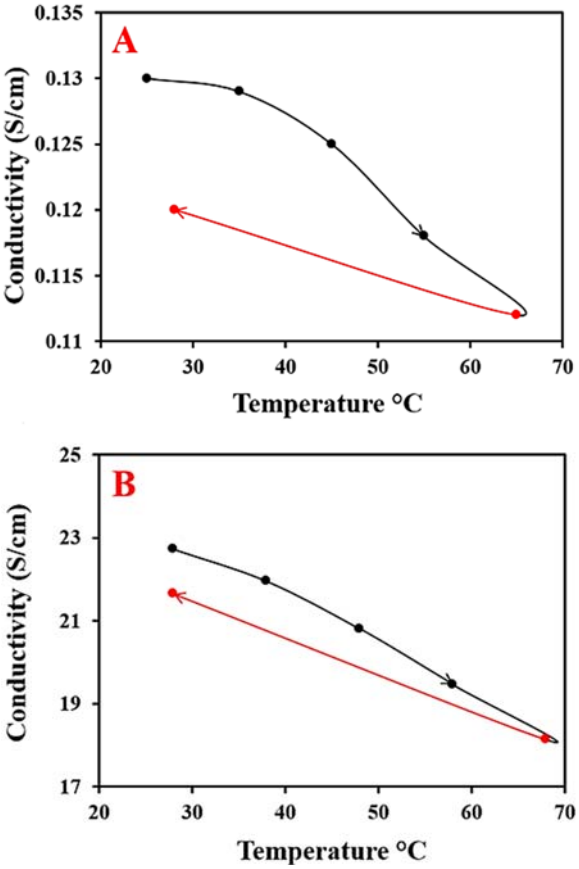

Fig. 8. The effect of temperature on the electrical conductivity of $PANI_{50\ wt\%}/PU$ (A) and $PANI_{75\ wt\%}/PU$ (B) materials.

As observed on pristine PANI(CSA) the electrical conductivity of the materials decreases with temperature increasing from 25 to 68 °C. This value changes from 0.13 to 0.11 S/cm between 25 and 65 °C for $PANI_{50\ wt\%}/PU$ and from 23 to 18 S/cm between 28 and 68 °C for $PANI_{75\ wt\%}/PU$. In fact, at higher temperatures the charge transport in the conductive phase is limited by the phonon scattering.

These variations are reversible: when the temperature is then decreasing to 28 °C, the

conductivity of $PANI_{50\ wt\%}$/PU and $PANI_{75\ wt\%}$/PU returns to 0.12 S/cm and 21.5 S/cm, respectively. Therefore, the materials were not damaged under the effect of the temperature. However, we can't necessarily associate the decrease of the electrical conductivity with the decrease of sensors sensitivity.

3.2. Detection of Ammonium Nitrate Particles

Sensors were then tested in the presence of ammonium nitrate particles between 270 µg.m^{-3} and 1100 µg.m^{-3} at 50 °C. The calibration curve of $PANI_{50\ wt\%}$/PU sensors obtained by plotting their relative response as a function of the concentration of ammonium nitrate particles is given in Fig. 9. The sensor showed a response of 2.2 % at 1100 µg.m^{-3} after 15 minutes of exposure, whereas sensor response at 270 µg/m^3 is around 1 %.

These results could be improved by reducing the relative humidity when particles are generated or by optimizing the decomposition temperature because high temperatures could accelerate the aging of sensitive surfaces. The kinetics of particles decomposition also depends on their diameter. Sufficient decomposition time is required. To achieve this, the particles were trapped in the exposure chamber during the heating period (15 minutes).

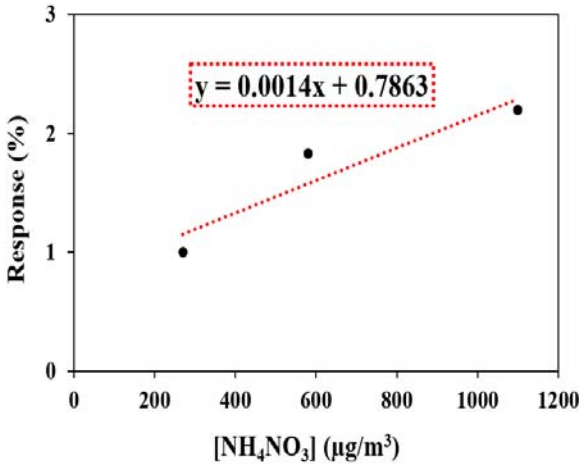

Fig. 9. Calibration curve of $PANI_{50\ wt\%}$/PU sensor in the presence of NH_4NO_3 particles (50°C/ particles trapped in the exposure chamber during 15 minutes).

Assuming that the sensor response to NH_4NO_3 particles is related to the released ammonia, then its concentration could be deduced from sensor sensitivity determined at 50 °C when the sensor is only exposed to ammonia and which is around 0.06 %.ppb^{-1} as given in Fig. 10. For the three mass concentrations of particles: 270 µg.m^{-3}, 580 µg.m^{-3} and 1100 µg.m^{-3}, the estimated concentrations of the released ammonia are: 17 ppb, 30 ppb and 37 ppb respectively.

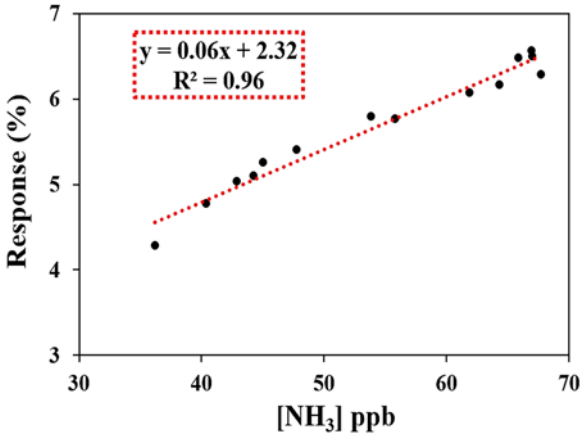

Fig. 10. Calibration curve and sensitivity of $PANI_{50\ wt\%}$/PU sensors to ammonia at 50 °C.

These concentrations were compared with the theoretical values of ammonia in equilibrium with ammonium nitrate particles at 50 °C and 45 % RH given by the dissociation constant K_p determined by Stelson and Seinfeld [29]. The dissociation constant of ammonium nitrate particles is expressed by the product of the concentrations of ammonia and nitric acid at equilibrium. It is estimated at 10^4 ppb at 50 °C which corresponds to 100 ppb of ammonia.

Assuming that 1 µg.m^{-3} of NH_4NO_3 gives 0.3 ppb of ammonia we can calculate the maximum concentration of NH_4NO_3 that could be dissociated at 50 °C and releases 100 ppb of ammonia. This concentration is estimated at 333 µg.m^{-3}. Therefore, at concentrations of NH_4NO_3 above 333 µg.m^{-3} the concentration of the released ammonia is 100 ppb. Whereas, below 333 µg.m^{-3} the concentration of the released ammonia is determined by multiplying the concentration of NH_4NO_3 by 0.3. Indeed, the theoretical concentration of ammonia is 81 ppb for 270 µg.m^{-3} of particles, and 100 ppb for both concentrations 580 µg.m^{-3} and 1100 µg.m^{-3}.

The experimental values are 3 to 5 times lower than the theoretical ones. Those differences can be explained by a lower particle decomposition under experimental conditions and/or by a competitive effect between the released nitric acid and the ammonia on the response of the sensor. Contrary to ammonia, the nitric acid can dope the PANI and reduce the sensor response to the target gas.

In the next step, ammonia concentrations deduced from sensor sensitivity to ammonia at 50°C should be compared with ammonia concentrations measured by another reference method to verify if sensor sensitivity has been influenced by the released nitric acid. The sensor should be then characterized in the presence of nitric acid in order to extract its response to ammonia.

4. Conclusions

Using ammonia sensitive surfaces based on polyaniline nanocomposites, we have proposed low-

cost sensors for simultaneous and selective measurement of ammonium nitrate particles and its gaseous precursor ammonia. The sensitive surfaces were synthesized with polyaniline associated with polyurethane. The first results obtained in the presence of ammonia showed a good sensitivity of PANI/PU materials at concentrations less than 60 ppb (around 0.33 %.ppb^{-1}) with limit of detection lower than 20 ppb. Moreover, good repeatability and reproducibility were obtained. PANI/PU sensors characterized in the presence of ammonium nitrate particles at 50 °C, were capable of measuring a concentration of ammonium nitrate particles as low as 270 µg.m^{-3} with a sensitivity of 0.0014 %.µg^{-1}.m^3. The ongoing work is focused on the characterization of PANI/PU materials at lower concentrations of NH_4NO_3 particles.

Acknowledgements

The authors are thankful to ADEME (Agence de l'Environnement et de la Maîtrise de l'Energie) in France for supporting this project and co-financing the PhD thesis of Mr. Mohamed BOUKHENANE with Région Hauts-de-France. The authors acknowledge also the staff of "SENSORS laboratory" and CERI (Centre d'Enseignement, de Recherche et d'Innovation) Energy and Environment of Institut Mines-Télécom Lille Douai (France).

References

[1]. V. P. Aneja, J. P. Chauhan, J. T. Walker, Characterization of atmospheric ammonia emissions from swine waste storage and treatment lagoons, *J. Geophys. Res. Atmospheres*, Vol. 105, Issue D9, 2000, pp. 11535–11545.

[2]. J. H. Seinfeld, S. N. Pandis, Atmospheric Chemistry and Physics: From Air Pollution to Climate Change, *John Wiley & Sons*, 2016.

[3]. K. W. Van Der Hoek, Estimating ammonia emission factors in Europe: Summary of the work of the UNECE ammonia expert panel, *Atmos. Environ.*, Vol. 32, Issue 3, 1998, pp. 315–316.

[4]. A. Fangmeier, A. Hadwiger-Fangmeier, L. Van der Eerden, H.-J. Jäger, Effects of atmospheric ammonia on vegetation-A review, *Environ. Pollut.*, Vol. 86, Issue 1, 1994, pp. 43–82.

[5]. X. Tang, X. Zhang, Z. Ci, J. Guo, J. Wang, Speciation of the major inorganic salts in atmospheric aerosols of Beijing, China: Measurements and comparison with model, *Atmos. Environ.*, Vol. 133, 2016, pp. 123–134.

[6]. T. Li, R. Hu, Z. Chen, Q. Li, S. Huang, Z. Zhu, L.-F. Zhou, Fine particulate matter ($PM_{2.5}$): The culprit for chronic lung diseases in China, *Chronic Dis. Transl. Med.*, Vol. 4, Issue 3, 2018, pp. 176–186.

[7]. X. Querol, A. Alastuey, T. Moreno, M. M. Viana, S. Castillo, J. Pey, S. Rodríguez, B. Artiñano, P. Salvador, M. Sánchez, S. Garcia Dos Santos, M. D. Herce Garraleta, R. Fernandez-Patier, S. Moreno-Grau, L. Negral, M. C. Minguillón, E. Monfort, M. J. Sanz, R. Palomo-Marín, E. Pinilla-Gil, E. Cuevas, J. de la Rosa, A. Sánchez de la Campa, Spatial and temporal variations in airborne particulate matter (PM_{10} and $PM_{2.5}$) across Spain 1999–2005, *Atmos. Environ.*, Vol. 42, Issue 17, 2008, pp. 3964–3979.

[8]. N. Amil, M. T. Latif, M. F. Khan, M. Mohamad, Seasonal variability of $PM_{2.5}$ composition and sources in the Klang Valley urban-industrial environment, *Atmospheric Chem. Phys.*, Vol. 16, Issue 8, 2016, pp. 5357–5381.

[9]. J. Hu, Y. Wang, Q. Ying, H. Zhang, Spatial and temporal variability of $PM_{2.5}$ and PM_{10} over the North China Plain and the Yangtze River Delta, China, *Atmos. Environ.*, Vol. 95, 2014, pp. 598–609.

[10]. D. Lv, Y. Chen, T. Zhu, T. Li, F. Shen, X. Li, Tariq Mehmood, The pollution characteristics of PM_{10} and $PM_{2.5}$ during summer and winter in Beijing, Suning and Islamabad, *Atmospheric Pollut. Res.,* Vol. 10, Issue 4, 2019, pp. 1159-1164.

[11]. Y. Wang, Y. Ma, Z. Lu, H. Ma, Y. Zhang, N. Liu, Y. Hong, X. Li, In situ measurement of atmospheric particles mass concentration in Anshan, in *Proceedings of the IOP Conf. Ser. Earth Environ. Sci.*, Vol. 69, Issue 1, 2017, 012026.

[12]. S. K. Sharma, T. K. Mandal, Chemical composition of fine mode particulate matter ($PM_{2.5}$) in an urban area of Delhi, India and its source apportionment, *Urban Clim.*, Vol. 21, 2017, pp. 106–122.

[13]. J. Tao, L. Zhang, G. Engling, R. Zhang, Y. Yang, J. Cao, C. Zhu, Q. Wang, L. Luo, Chemical composition of $PM_{2.5}$ in an urban environment in Chengdu, China: Importance of springtime dust storms and biomass burning, *Atmospheric Res.*, Vol. 122, 2013, pp. 270–283.

[14]. L. He, H. Chen, J. Rangognio, A. Yahyaoui, P. Colin, J. Wang, V. Daële, A. Mellouki, Fine particles at a background site in Central France: Chemical compositions, seasonal variations and pollution events, *Sci. Total Environ.*, Vol. 612, 2018, pp. 1159–1170.

[15]. D. Salameh, A. Detournay, J. Pey, N. Pérez, F. Liguori, D. Saraga, M.C. Bove, P. Brotto, F. Cassola, D. Massabò, A. Latella, S. Pillon, G. Formenton, S. Patti, A. Armengaud, D. Piga, J.L. Jaffrezo, J. Bartzis, E. Tolis, P. Prati, X. Querol, H. Wortham, N. Marchand, $PM_{2.5}$ chemical composition in five European Mediterranean cities: A 1-year study, *Atmospheric Res.*, Vol. 155, 2015, pp. 102–117.

[16]. H. Wang, X. Li, G. Shi, J. Cao, C. Li, F. Yang, Y. Ma, K. He, $PM_{2.5}$ Chemical Compositions and Aerosol Optical Properties in Beijing during the Late Fall, *Atmosphere*, Vol. 6, Issue 2, 2015, pp. 164–182.

[17]. N. Jiang, S. Yin, Y. Guo, J. Li, P. Kang, R. Zhang, X. Tang, Characteristics of mass concentration, chemical composition, source apportionment of $PM_{2.5}$ and PM_{10} and health risk assessment in the emerging megacity in China, *Atmospheric Pollut. Res.,* Vol. 9, Issue 2, 2018, pp. 309–321.

[18]. A. W. Stelson, S. K. Friedlander, J. H. Seinfeld, A note on the equilibrium relationship between ammonia and nitric acid and particulate ammonium nitrate, *Atmospheric Environ. 1967*, Vol. 13, Issue 9, 1979, pp. 369–371.

[19]. C. B. Richardson, R. L. Hightower, Evaporation of ammonium nitrate particles, *Atmospheric Environ. 1967*, Vol. 21, Issue 4, 1987, pp. 971–975.

[20]. R. K. Pathak, W. S. Wu, T. Wang, Summertime $PM_{2.5}$ ionic species in four major cities of China: nitrate

formation in an ammonia-deficient atmosphere, *Atmos. Chem. Phys.,* Vol. 9, 2009, pp. 1711–1720.

[21]. Y. Tao, X. Ye, Z. Ma, Y. Xie, R. Wang, J. Chen, X. Yang, S. Jiang, Insights into different nitrate formation mechanisms from seasonal variations of secondary inorganic aerosols in Shanghai, *Atmos. Environ.,* Vol. 145, 2016, pp. 1–9.

[22]. X. Zhang, P. H. McMurry, Evaporative losses of fine particulate nitrates during sampling, *Atmospheric Environ. Part Gen. Top.*, Vol. 26, Issue 18, 1992, pp. 3305–3312.

[23]. D. H. Lowenthal, N. Kumar, $PM_{2.5}$ Mass and Light Extinction Reconstruction in IMPROVE, *J. Air Waste Manag. Assoc.,* Vol. 53, Issue 9, 2003, pp. 1109–1120.

[24]. F. M. Kelly, L. Meunier, C. Cochrane, V. Koncar, Polyaniline: Application as solid state electrochromic in a flexible textile display, *Displays,* Vol. 34, Issue 1, 2013, pp. 1–7.

[25]. S. Mikhaylov, N. Ogurtsov, Y. Noskov, N. Redon, P. Coddeville, J.-L. Wojkiewicz, A. Pud, Ammonia/amine electronic gas sensors based on hybrid polyaniline–TiO_2 nanocomposites. The effects of titania and the surface active doping acid, *RSC Adv.*, Vol. 5, Issue 26, 2015, pp. 20218–20226.

[26]. J. L. Wojkiewicz, V. N. Bliznyuk, S. Carquigny, N. Elkamchi, N. Redon, T. Lasri, A. A. Pud, S. Reynaud, Nanostructured polyaniline-based composites for ppb range ammonia sensing, *Sens. Actuators B Chem.,* Vol. 160, Issue 1, 2011, pp. 1394–1403.

[27]. M. L. Boukhenane, N. Redon, J. L. Wojkiewicz, P. Coddeville, Polyaniline nanocomposites based sensor for simultaneous and selective measurement of ammonium nitrate aerosol and ammonia gas, in *Proceedings of the 5th International Conference on Sensors Engineering and Electronics Instrumentation Advances (SEIA'19),* Tenerife (Canary Islands), Spain, 25-27 September 2019, pp. 250–254.

[28]. A. L. Kukla, Y. M. Shirshov, S. A. Piletsky, Ammonia sensors based on sensitive polyaniline films, *Sens. Actuators B Chem.,* Vol. 37, Issue 3, 1996, pp. 135–140.

[29]. A. W. Stelson, J. H. Seinfeld, Relative humidity and temperature dependence of the ammonium nitrate dissociation constant, *Atmospheric Environ. 1967*, Vol. 16, Issue 5, 1982, pp. 983–992.

[30]. T. Mérian, N. Redon, Z. Zujovic, D. Stanisavljev, J. L. Wojkiewicz, M. Gizdavic-Nikolaidis, Ultra sensitive ammonia sensors based on microwave synthesized nanofibrillar polyanilines, *Sens. Actuators B Chem.,* Vol. 203, 2014, pp. 626–634.

[31]. S. Bai, Y. Tian, M. Cui, J. Sun, Y. Tian, R. Luo, A. Chen, D. Li, Polyaniline@SnO_2 heterojunction loading on flexible PET thin film for detection of NH_3 at room temperature, *Sens. Actuators B Chem.,* Vol. 226, 2016, pp. 540–547.

[32]. S. B. Kulkarni, Y. H. Navale, S. T. Navale, N. S. Ramgir, A. K. Debnath, S. C. Gadkari, S. K. Gupta, D. K. Aswal, V. B. Patil, Enhanced ammonia sensing characteristics of tungsten oxide decorated polyaniline hybrid nanocomposites, *Org. Electron.,* Vol. 45, 2017, pp. 65–73.

[33]. H. Tai, Y. Jiang, G. Xie, J. Yu, X. Chen, Fabrication and gas sensitivity of polyaniline–titanium dioxide nanocomposite thin film, *Sens. Actuators B Chem.,* Vol. 125, Issue 2, 2007, pp. 644–650.

[34]. Y. Li, H. Ban, H. Zhao, M. Yang, Facile preparation of a composite of TiO_2 nanosheets and polyaniline and its gas sensing properties, *RSC Adv.,* Vol. 5, Issue 129, 2015, pp. 106945–106952.

[35]. X. Wang, S. Meng, M. Tebyetekerwa, W. Weng, J. Pionteck, B. Sun, Z. Qin, M. Zhu, Nanostructured polyaniline/poly(styrene-butadiene-styrene) composite fiber for use as highly sensitive and flexible ammonia sensor, *Synth. Met.,* Vol. 233, 2017, pp. 86–93.

[36]. L. Xue, W. Wang, Y. Guo, G. Liu, P. Wan, Flexible polyaniline/carbon nanotube nanocomposite film-based electronic gas sensors, *Sens. Actuators B Chem.,* Vol. 244, 2017, pp. 47–53.

[37]. Z. Wu, X. Chen, S. Zhu, Z. Zhou, Y. Yao, W. Quan, B. Liu, Enhanced sensitivity of ammonia sensor using graphene/polyaniline nanocomposite, *Sens. Actuators B Chem.,* Vol. 178, 2013, pp. 485–493.

[38]. D. K. Bandgar, S. T. Navale, S. R. Nalage, R. S. Mane, F. J. Stadler, D. K. Aswal, S. K. Gupta, V. B. Patil, Simple and low-temperature polyaniline-based flexible ammonia sensor: a step towards laboratory synthesis to economical device design, *J. Mater. Chem. C.,* Vol. 3, Issue 36, 2015, pp. 9461–9468.

[39]. Z. Pang, Z. Yang, Y. Chen, J. Zhang, Q. Wang, F. Huang, Q. Wei, A room temperature ammonia gas sensor based on cellulose/TiO_2/PANI composite nanofibers, *Colloids Surf. Physicochem. Eng. Asp.,* Vol. 494, 2016, pp. 248–255.